Rivista Italiana di Paleontologia e Stratigrafia
(*Research in Paleontology and Stratigraphy*)
vol. 127(3): 539-556. **November 2021**

HIGH-RESOLUTION CALCAREOUS NANNOFOSSIL BIOSTRATIGRAPHY ACROSS THE TOARCIAN OCEANIC ANOXIC EVENT IN NORTHERN ITALY: CLUES FROM THE SOGNO AND GAJUM CORES (LOMBARDY BASIN, SOUTHERN ALPS)

STEFANO VISENTIN[1] & ELISABETTA ERBA[1*]

[1]Dipartimento di Scienze della Terra "Ardito Desio", Università degli Studi di Milano, Via Mangiagalli 34, 20133 Milano, Italy.
*Corresponding Author. E-mail: elisabetta.erba@unimi.it.

To cite this article: Visentin S. & Erba E. (2021) - High-resolution calcareous nannofossil biostratigraphy across the Toarcian Oceanic Anoxic Event in Northern Italy: clues from the Sogno and Gajum Cores (Lombardy Basin, Southern Alps). *Riv. It. Paleontol. Strat.,* 127(3): 539-556.

Keywords: Calcareous nannofossils; biostratigraphy; Toarcian Oceanic Anoxic Event; Lombardy Basin.

Abstract: Calcareous nannofossil biostratigraphy was conducted across the Toarcian Oceanic Anoxic Event (T-OAE) interval cored at Colle di Sogno and Gajum in the Lombardy Basin (Southern Alps, Northern Italy). Drilling at both sites resulted in 100% recovery of unweathered material. The Sogno and Gajum Cores consist of pelagic marly limestones, marlstone, marly claystone, and a relatively expanded black shale interval named Fish Level considered the lithostratigraphic record of the T-OAE at regional scale.

Semiquantitative analyses of calcareous nannofloras allowed to achieve a high-resolution biostratigraphy of the latest Pliensbachian-early Toarcian time interval. Several nannofossil biohorizons were detected, including zonal/subzonal markers and additional events related to changes in abundance. The nannofossil biostratigraphic correlation of the Sogno and Gajum Cores indicates that, according to their paleogeographic settings, the succession recovered in the Sogno Core deposited on a pelagic plateau is continuous while a hiatus of ~600 kyrs was detected in the lowermost Toarcian in the Gajum Core located on a slope of a structural high.

The NJT 5 and NJT 6 Zones of the standard nannofossil zonation for the Mediterranean Province were identified in both the Sogno and Gajum Cores. Our findings allow an implementation of the reference biozonation with the separation of the NJT 6a and NJT 6b Subzones, and age revision of some secondary events. The zonation established for the Lusitanian Basin (Portugal) is only partially reproducible in the Lombardy Basin, confirming nannoplankton paleoprovincialism during the Early Jurassic requiring different zonal schemes in various areas. Nevertheless, we underline that the T-OAE is unambiguously constrained by the FO of *C. superbus crassus* and the LO of *M. jansae* at supra-regional scale.

Introduction

The early Toarcian Oceanic Anoxic Event (T-OAE) is recognized as one of the most severe and geographically widespread events of oceanic anoxia and organic-carbon burial in the Mesozoic (Jenkyns 1985, 1988, 2003, 2010). Coeval paleoenvironmental perturbations have been linked to volcanism of the Karoo-Ferrar Large Igneous Province (LIP) and its release of volcanogenic CO_2, and/or thermogenic methane (CH_4) from sill intrusion into Gondwanan coals, and/or biogenic methane from dissociation of sub-seafloor clathrates (Hesselbo et al. 2000; Kemp et al. 2005; McElwain et al. 2005; Svensen et al. 2007; Jenkyns 2010; Reolid et al. 2020). This dramatic episode of ecosystem adjustments, global warming and altered ocean chemistry occurred during a crucial time for calcareous nannoplankton diversification as a major speciation episode took place in the late Pliensbachian-early Toarcian time interval (Bown 1987; Mattioli & Erba 1999; Bown

Received: January 14, 2021; accepted: June 25, 2021

et al. 2004; Erba 2004, 2006; Fraguas & Young 2011; Menini et al. 2019). New genera and species appeared and quickly evolved allowing a high-resolution biostratigraphy also across the T-OAE (Mattioli & Erba 1999; Mattioli et al. 2004; Casellato & Erba 2015; Ferreira et al. 2019). Moreover, major changes in abundance of some taxa were proved coeval in the late Pliensbachian-early Toarcian time interval and probably related to large scale paleoenvironmental stress preceding and across the T-OAE (Erba 2004; Mattioli et al. 2004, 2008; Tremolada et al. 2005; Fraguas et al. 2012; Casellato & Erba 2015; Clémence et al. 2015; Menini et al. 2019; Visentin et al. 2021b). Calcareous nannofossils were proved to be extremely useful for high-resolution biostratigraphic dating and correlations at low, medium, and high latitudes. Two standard biozonations are available for the Early Jurassic: the one of Bown (1987) revised by Bown & Cooper (1998) established for the Boreal Realm (United Kingdom, Germany, The Netherlands, central and Northern France) and the zonal scheme of Mattioli & Erba (1999) specific for the Tethyan area (Italy, Southern and Eastern Spain, South France, Hungary, Greece). More recently, two zonal schemes were published for the Cantabrian Range in Northern Spain (Fraguas et al. 2015, 2018) and the Lusitanian Basin in Portugal (Ferreira et al. 2019).

Calcareous nannofossil biostratigraphy across the T-OAE has been documented for several outcrop sections (see Ferreira et al. 2019 for a review) and a few cores (Van de Schootbrugge et al. 2019; Visentin et al. 2021b). Core successions are, in many cases, preferable since unweathered lithologies usually display a much better preservation and sampling can be conducted in much higher resolution resulting in a more resolved taxonomy and biostratigraphy. The Sogno and Gajum drilling project was, in fact, aimed at recovering high-resolution data from continuous and well-preserved sequences since outcropping sedimentary rocks, and particularly black shales, are commonly badly degraded (Erba et al. 2019b). Continuous coring is, thus, crucial to recover high-quality fresh material with potentially good preservation.

In this work we present a detailed calcareous nannofossil biostratigraphy of two continuously cored successions representing significantly different geological settings within the Lombardy Basin (Southern Alps) (Erba et al. 2019b). The Sogno Core was drilled on the Albenza Plateau (a pelagic structural high) while the Gajum Core was penetrated in an inner basin along the slope of the Mt. Corni di Canzo structural high (Fig. 1). Both cores recovered a pelagic succession through the uppermost portion of the Domaro Limestone (Lmst.) and the lower part of Sogno Formation (Fm.) including the Fish Level, which represents the lithological expression of the T-OAE in the Lombardy Basin (Tintori 1977; Gaetani & Poliani 1978; Erba & Casellato 2010; Erba et al. 2019a, b).

The calcareous nannofossil biostratigraphic investigation of the Sogno and Gajum Cores is aimed at building a robust framework to constrain the T-OAE paleoenvironmental changes at local, regional, and supra-regional scale. In particular, nannofossil events will be used to date the Fish Level black shale interval pointing out synchroneity or diachroneity within the Lombardy Basin, and also for comparison with other basins at different latitudes. Analogies and differences will be used to derive reproducibility and lateral extension of calcareous nannofossil events.

GEOLOGICAL SETTING AND LITHOSTRATIGRAPHY

During the Jurassic, the Lombardy Basin was a relatively deep area bordered by the Canavese Zone to the West and the Trento Plateau to the East (Gaetani 1975; 2010; Bernoulli & Jenkyns 2009). During latest Triassic to earliest Jurassic times, a rifting phase broke the southern margin of the Western Tethys into depressions and paleohighs that are, from West to East: Monte Nudo Trough, Lugano High, Generoso Trough, Corni di Canzo High, Albenza Plateau, Monte Cavallo High, Sebino Trough, Botticino High (Gaetani 1975, 2010) (Fig. 1). In the troughs, Lower Jurassic partially resedimented sequences may reach a non-decompacted thickness of 3000 m (e.g., in the Generoso Trough), while condensation and/ or hiatuses distinguish the paleohigh successions, often represented by reddish nodular facies. On the escarpments connecting the highs to the deeper parts, sedimentation was affected by slumps, resedimented intervals and locally submarine breccias, typically interrupting condensed and seldom incomplete successions (Gaetani & Erba 1990;

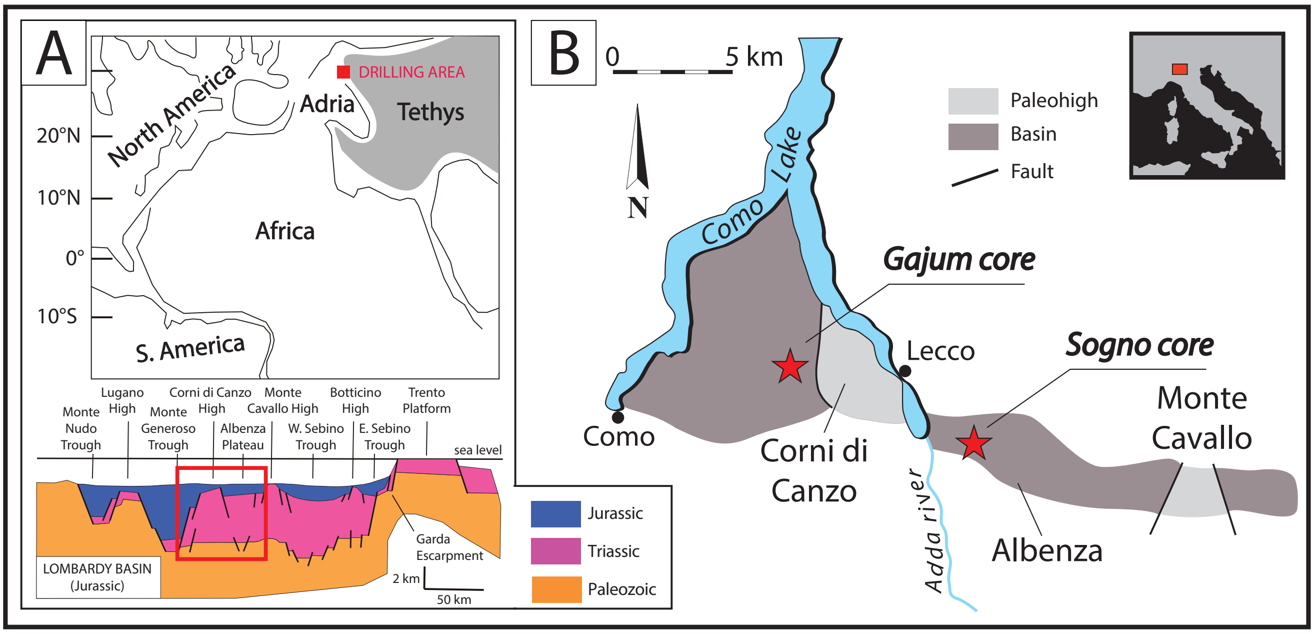

Fig. 1 - Location of the Sogno and Gajum drilling sites relative to A) paleo- and B) current geography (after Erba et al. 2019b).

Gaetani 2010) (Fig. 1). The Lower Jurassic successions of the Lombardy Basin were influenced by local-regional tectonics, but also shaped by global paleoenvironmental perturbations including the T-OAE (Erba et al. 2019a). Lower Toarcian sections contain a distinctive black shale interval that is the sedimentary record of oxygen-depleted seafloor of the Tethys Ocean. In the Lombardy Basin the lower Toarcian black shale interval was named Livello a Pesci/Fish Level (Tintori 1977): it generally has a thickness between 0.5 and 5 m, but can reach a few tens of meters in the most expanded sections. Black shales are ubiquitous in the deeper settings of the Lombardy Basin, but are commonly absent on paleo-highs (tops and upper slopes), usually resulting from stratigraphic gaps and/or extreme condensation.

The Colle di Sogno and Gajum sites were selected as pelagic records (Gaetani & Erba 1990; Casellato & Erba 2015) for continuous coring of the lower Toarcian Fish Level. Within the Lombardy Basin, these sites represent different depositional settings on a pelagic structural high (Albenza Plateau) and in an inner basin along the slope of a structural high (Mt. Corni di Canzo). At both locations, the Fish Level is present in the lower part of the Sogno Formation (Gaetani & Poliani 1978; Gaetani & Erba 1990; Casellato & Erba 2015) providing the opportunity to date, investigate and model the anoxic interval.

At Colle di Sogno, the type-section of the Sogno Fm. was formalized along the road SP 179 on the northern slope of Mt. Brughetto (Gaetani & Poliani 1978). The pelagic calcilutites of the Domaro Limestone (Lmst.) Fm. are suddenly followed by the Sogno Fm. consisting of marlstones, calcareous marlstones, marly limestones, and black shales. The upper Pliensbachian-lower Bajocian Colle di Sogno section was characterized stratigraphically through litho-, bio-, chemo-, magneto-, and cyclostratigraphy (Gaetani & Poliani 1978; Jenkyns & Clayton 1986; Gaetani & Erba 1990; Hinnov et al. 2000; Channell et al. 2010; Casellato & Erba 2015). The Gajum outcrop is located in a small lateral cut of the Ravella Valley (close to the Canzo village), where the carbonate-rich lithologies of the Domaro Lmst. are followed by dark grey, clay-rich lithologies of the Sogno Fm. overlain by reddish nodular limestones of the Rosso Ammonitico Lombardo.

Erba et al. (2019b) described in detail the lithostratigraphy of the Sogno and Gajum Cores. Lithologic units were defined taking into account lithological features and sedimentary structures. For each core, at least four dip measurements were taken during lab preparation to calculate the stratigraphic thickness of the drilled sections. The composite Sogno Core section recovered a complete upper Pliensbachian–lower Toarcian interval (total stratigraphic thickness = 25.33 m) represented by the uppermost part of the Domaro Lmst. and the lower part of the

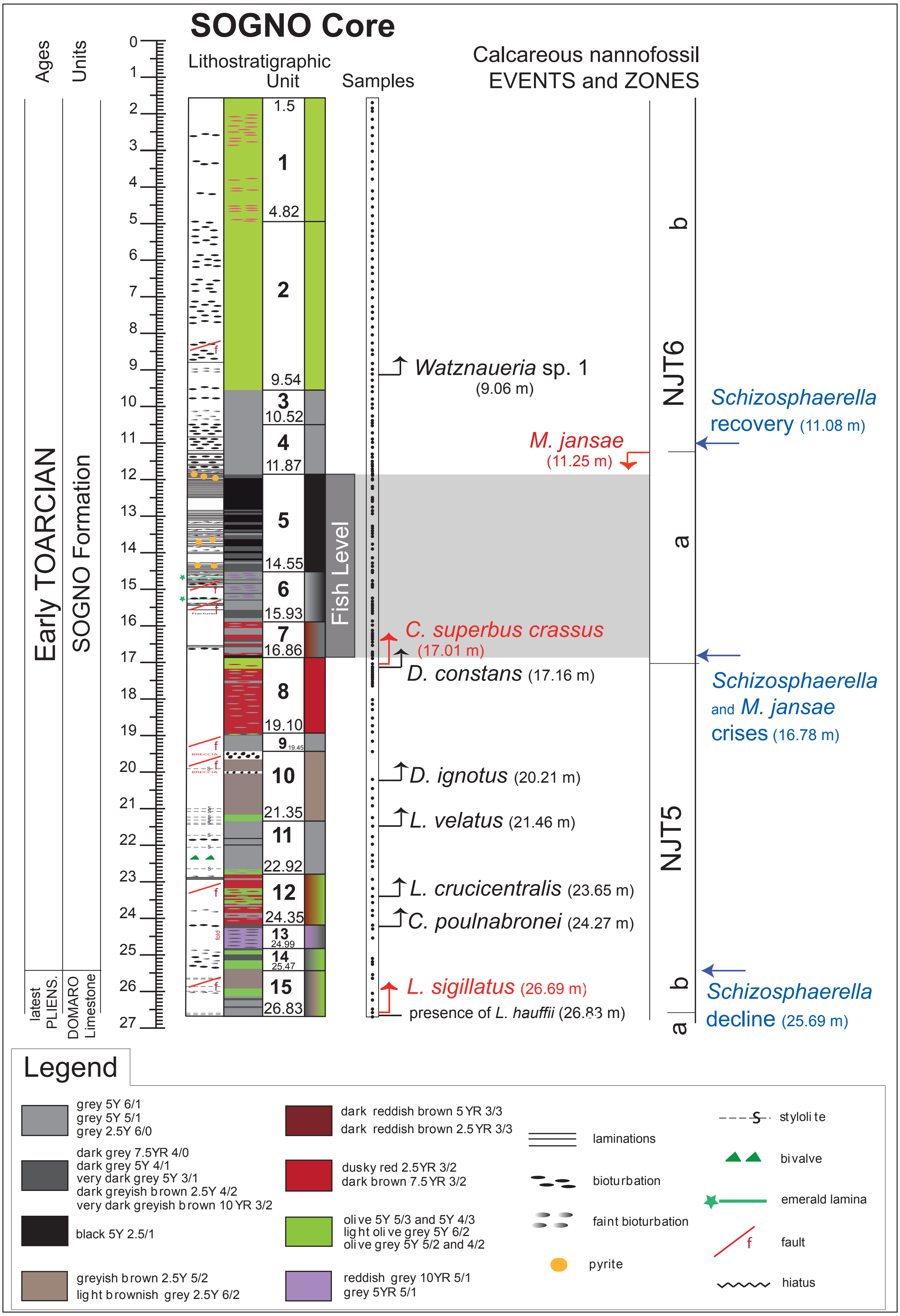

Fig. 2 - Lithostratigraphy and biostratigraphy of the Sogno Core. Calcareous nannofossil events in red are the primary events used as zonal and subzonal boundaries. The *Schizosphaerella* decline, crisis, recovery, and *M. jansae* crisis are reported in blue.

Sogno Fm. (Fig. 2). The Gajum Core recovered the Domaro Lmst. immediately overlain by the Fish Level black shales, followed by marlstones of the Sogno Fm. and the Rosso Ammonitico Lombardo (total stratigraphic thickness = 28.18 m) (Fig. 3).

MATERIALS AND METHODS

A total of 154 samples were selected for calcareous nannofossil biostratigraphy of the Sogno Core. The average sampling rate adopted is 16 cm through the core succession: the lowermost 9 m (core bottom to lower unit 8) and the uppermost 9 m (upper part of unit 4 to core top) were sampled at a slightly lower resolution of 20 cm whereas the Fish Level and the interval immediately preceding and following (upper part of unit 8, units 7, 6, 5 and lower part of unit 4) were sampled every 10 cm (Fig. 2). Biostratigraphic analyses were performed on smear slides prepared following the settling boxes method of Geisen et al. (1999) that was applied to conduct future quantitative investigations. According to this technique, a basic pH suspension of 0.1 g of dried rock powder and ammoniac water was homogenized and let settled for 24 h on a cover slide in a settling device. The cover slide was recovered, dried, and attached to a slide with the Norland Optical Adhesive.

A total of 156 samples were collected from the Gajum Core. The average sampling rate adopted is 20 cm with the exception of the Domaro Lmst./Sogno Fm. lithostratigraphic boundary corresponding to the inception of the black shales of the Fish Level (lowermost unit 6) sampled every 0.5-1 cm (Fig. 3). Samples were prepared from limestones and marly limestones of the Domaro Lmst., limy marlstones, marlstones, marly claystones and black shales of the Sogno Fm. and nodular limestones of the Rosso Ammonitico Lombardo Fm. Simple smear slides were prepared following the method of Monechi & Thierstein (1985): a small amount of rock material was powdered adding few drops of bi-distillate water, without centrifuging, ultrasonic cleaning or settling the sediment in order to retain the original composition. The obtained suspension was mounted onto a slide, covered with a cover slide fixed with the Norland Optical Adhesive.

Smear slides of both cores were investigated using a light polarizing microscope, at 1250X magnification. Calcareous nannofossil abundance and preservation were evaluated by examining at least 6 longitudinal traverses (750 fields of view) in each smear slide. Preservation of calcareous nannofossils was characterized adopting the codes described by Roth (1983) for etching and overgrowth (see Appendices 2 and 3). For each sample, semi-quantitative abundances of individual taxa and total nannofossil assemblages were obtained as number of specimens in a microscope field of view as detailed in Appendices 2 and 3.

The biozonation scheme adopted is that of Mattioli & Erba (1999) established for the Tethyan Realm. Calcareous nannofossil taxa recognized in this study are listed in Appendix 1. The range charts of calcareous nannofossil taxa from the Sogno and Gajum Cores are reported in Appendices 2 and 3. Plates 1 and 2 contain the photographs of the most common taxa.

TAXONOMIC NOTES

In the present work we followed the recent taxonomic revision for the genus *Carinolithus* conducted by Visentin et al. (2021a). Specifically, morphometric analyses allowed the separation of *C. superbus crassus* from *C. superbus superbus* based on the stem width (SW). The former taxon has a SW > 1 μm whereas the latter is characterized by a SW ≤ 1 μm. As a consequence, Visentin et al. (2021a) concluded that *C. superbus,* whose FO is used as marker for the base of the NJ 6 and NJT 6 Zones in the reference biozonation schemes (Bown & Cooper 1998; Mattioli & Erba 1999; Ferreira et al. 2019), is indeed *C. superbus crassus*. Visentin et al. (2021a) further demonstrated that the species *C. cantaluppii* is a diagenetic artefact of *Carinolithus* specimens due to intensive overgrowth (highly calcified *C. poulnabronei* and *C. superbus*) and, accordingly, we disregard this taxon.

The taxonomic subdivisions of Casellato & Erba (2015) were applied as follows: a) *C. crassus* is subdivided into *C. crassus* (length ≥ 5 μm) and "small" *C. crassus* (length < 5 μm) ; b) *M. jansae* is divided into *M. jansae* and "thin" *M. jansae*; c) *S. punctulata* is divided into *S. punctulata*, "small" *S. punctulata* and "encrusted" *S. punctulata.* Additionally, similarly to Casellato & Erba (2015), we consider the taxon *Watznaueria* sp. 1 corresponding to *W. fossacincta* of Mattioli & Erba (1999) and Ferreira et al. (2019).

RESULTS

Calcareous nannofossil preservation and abundance

Calcareous nannofossil preservation and abundance vary through the studied interval, showing comparable and consistent variations in the two cores. In the Sogno Core the preservation is generally moderate to moderate/good varying from moderate/poor to moderate in the Domaro Lmst. and from moderate/poor to good in the Sogno Fm., with the exception of the Fish Level where a moderate/poor to moderate/good preservation was observed. The degree of etching varies from E1 to E2, with stronger dissolution within the Fish Level, whereas the degree of overgrowth fluctuates between O0 and O2 and is relatively higher in the Domaro Lmst. Similar results were obtained for the Gajum Core: a generally moderate preservation shows variations from poor to moderate/good in the Domaro Lmst. and within the Fish Level, moderate/poor to good in the uppermost part of the Sogno Fm. and from moderate/poor to moderate within the Rosso Ammonitico Lombardo Fm. The degree of etching varies from E1 to E3 and, as for the Sogno Core, stronger dissolution is observed within the Fish Level while the degree of overgrowth fluctuates between O0 and O3 with stronger evidence of overgrowth in the Domaro Lmst. and occasionally in the Rosso Ammonitico Lombardo Fm.

The calcareous nannofossil abundance is somehow lithology-dependent: nannofossils are rare to rare/frequent and rare/frequent to frequent in the Domaro Lmst. of the Sogno Core and Gajum Core, respectively. Within the Sogno Fm., nannofossils are generally frequent, fluctuating between rare to frequent/common in both cores. A drastic decrease in total abundance is observed in the Fish Level, characterized by extremely rare nannofossils with a few sporadic samples containing rare/frequent or frequent specimens. The Rosso Ammonitico Lombardo Fm. is characterized by rare/frequent to frequent nannofossils.

Biostratigraphy

Sogno Core

A total of nine calcareous nannofossil events were recognized in the Sogno Core (Fig. 2) and the NJT 5 (divided into the NJT 5a and NJT 5b Subzones) and NJT 6 Zones were identified.

According to the zonation of Mattioli & Erba (1999), the lowermost studied sample (26.83 m) is attributed to the NJT 5a Subzone for the presence of *Lotharingius hauffii* and the absence of *Lotharingius sigillatus*. The first occurrence (FO) of *L. sigillatus* at 26.69 m (sample S3-C-473) marks the boundary between the NJT 5a and the NJT 5b Subzones. Within the NJT 5b Subzone additional biohorizons were recognized, namely: the FOs of *Carinolithus poulnabronei* (24.27 m), *Lotharingius crucicentralis* (23. 65 m), *Lotharingius velatus* (21.46 m), *Discorhabdus ignotus* (20.21 m) and *Diductius constans* (17.16 m). The FO of *Carinolithus superbus crassus* (17.01 m) defines the base of the NJT 6 Zone. The last occurrence (LO) of *Mitrolithus jansae* (11.25 m) and the FO of *Watznaueria* sp.1 (9.06 m) were detected within the NJ 6 Zone. Following Ferreira et al. (2019), we use here the LO of *M. jansae* to separate the NJT 6a and NJT 6b Subzones (Fig. 2). The NJT 6/NJT 7 zonal boundary was not identified because *Discorhabdus striatus* was not observed in the studied interval.

Variations in semiquantitative abundance of a few taxa were recorded (see range chart in Appendix 2) and previously defined acme-paracme levels were identified. Casellato & Erba (2015) identified the *Schizosphaerella* decline, crisis and recovery as well as the *M. jansae* crisis on the basis of absolute abundances obtained from ultrathin section analyses. However, semiquantitative analyses (Casellato & Erba 2015; Visentin et al. 2021b; this work) also allow the identification of the above mentioned biohorizons. In the Sogno Core, the *Schizosphaerella* decline corresponds to a change from common to frequent abundance at the Domaro Lmst./Sogno Fm. boundary (25.69 m); the *Schizosphaerella* and *M. jansae* crises are marked by a change from frequent and continuous records to rare and discontinuous occurrences and correlate with the base of the Fish Level (16.78 m). The *Schizosphaerella* recovery has been detected at the level where this taxon returns to be continuous and rare/frequent above the Fish Level (11.08 m) (Fig. 2).

The calcareous nannofossil assemblages of the NJT 5b Subzone are dominated by *Schizosphaerella punctulata* and *M. jansae*. Among schizosphaerellids, *S. punctulata* is the most abundant taxon (rare to common) whereas "small" *S. punctulata* (extremely rare to frequent/common) and "encrusted" *S. punctulata* (extremely rare to rare/frequent) are subordinated. Within genus *Mitrolithus, M. jansae* is slightly more abundant (extremely rare to frequent/common) than "thin" *M. jansae* (extremely rare to rare/frequent). Within genus *Lotharingius* a slight increase in abundance is observed for *L. hauffii, L. frodoi* and *L. sigillatus* in the upper part of the NJ 5b Subzone.

Nannofossil assemblages in the lower part of the NJT 6a Subzone, largely corresponding to the Fish Level, show a severe reduction in abundance of both *Schizosphaerella* and *Mitrolithus (Schizosphaerella* and *M. jansae* crises). In particular, both *S. punctulata* and "small" *S. punctulata* become extremely rare, and "encrusted" *S. punctulata* is recorded only sporadically. As far as *M. jansae* is concerned, abundances become rare to extremely rare and discontinuous in the Fish Level, with a bigger drop in abundance of the normal morphotype.

In the Fish Level *Lotharingius* becomes the dominant genus with *L. hauffii, L. frodoi* and *L. sigillatus* as most abundant species. In this interval, an increase in abundance for genera *Calyculus* and *Carinolithus* was also recorded (see range chart in Appendix 2).

Calcareous nannofossil assemblages of the uppermost part of the NJT 6a Subzone are characterized by a relative recovery of schizosphaerellids (*Schizosphaerella* recovery) above the Fish Level, although with limited abundance: *S. punctulata* is extremely rare to frequent and "small" *S.punctulata* is extremely rare to rare/frequent whereas "encrusted" *S. punctulata* remains sporadic.

Through the Sogno Core, genera *Biscutum*, *Calyculus, Carinolithus* and *Crepidolithus* are characterized by a general rare abundance, whereas *Bussonius*, *Diductius*, *Similiscutum, Parhabdolithus* and *Tubirhabdus* are extremely rare.

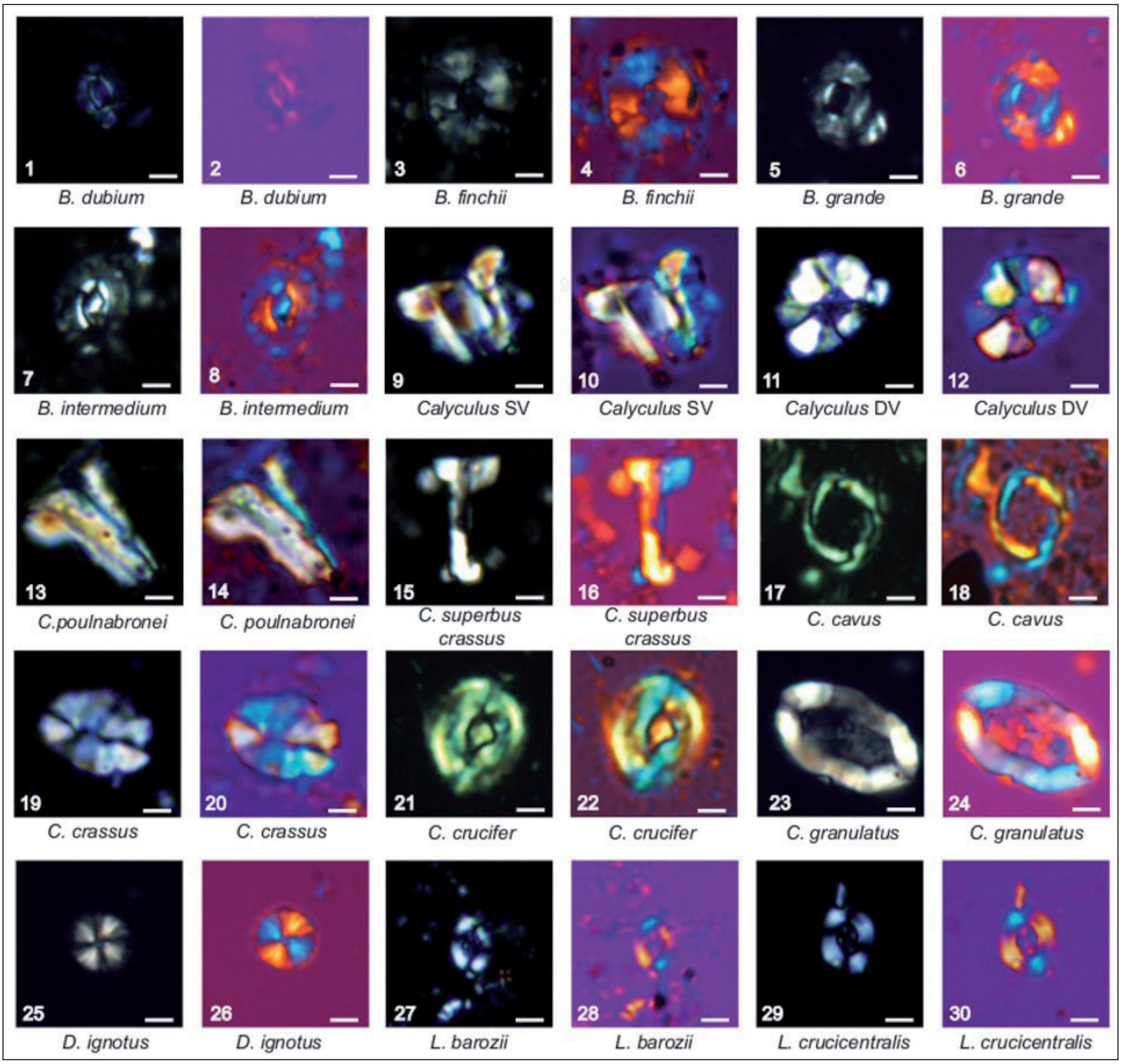

PLATE 1

Scale bars represent 2 μm.

1-2 - *B. dubium,* 1) cross-polarized light, 2) quartz lamina, Gajum Core, sample G C25 995 (26.94 m)
3-4 - *B. finchii*, 3) cross-polarized light, 4) quartz lamina, Sogno Core, sample S3 C12 330 (17.16 m)
5-6 - *B. grande*, 5) cross-polarized light, 6) quartz lamina, Gajum Core, sample G C25 994 (26.89 m)
7-8 - *B. intermedium*, 7) cross-polarized light, 8) quartz lamina, Sogno Core, sample S3 C12 330 (17.16 m)
9-10 - *Calyculus* spp. side view (SV), 9) cross-polarized light, 10) quartz lamina, Sogno Core, sample S3 C29 456 (25.5 m)
11-12 - *Calyculus* spp. distal view (DV), 11) cross-polarized light, 12) quartz lamina, Sogno Core, sample S3 C21 416 (22.95 m)
13-14 - *C. poulnabronei*, 13) cross-polarized light, 14) quartz lamina, Sogno Core, sample S3 C22 423 (23.42 m)
15-16 - *C. superbus crassus,* 15) cross-polarized light, 16) quartz lamina, Sogno Core, sample S3 C5 313 (13.42 m)
17-18 - *C. cavus,* 17) cross-polarized light, 18) quartz lamina, Gajum Core, sample G C16 623 (17.15 m)
19-20 - *C. crassus,* 19) cross-polarized light, 20) quartz lamina, Gajum Core, sample G C22 841 (23.09)
21-22 - *C. crucifer,* 21) cross-polarized light, 22) quartz lamina, Sogno Core, sample S1 C32 192 (11.86 m)
23-24 - *C. granulatus,* 23) cross-polarized light, 24) quartz lamina, Gajum Core, sample G C25 992 (26.85 m)
25-26 - *D. ignotus,* 25) cross-polarized light, 26) quartz lamina, Sogno Core, sample S3 C14 343 (17.9 m)
27-28 - *L. barozii,* 27) cross-polarized light, 28) quartz lamina, Gajum Core, sample G C7 275 (9. 15 m)
29-30 - *L. crucicentralis,* 29) cross-polarized light, 30) quartz lamina, Sogno Core sample S1 C7 35 (4.24 m)

Gajum Core

The calcareous nannofossil biostratigraphic investigation of the Gajum Core resulted in the identification of seven events and of the NJT 5 and NJT 6 Zones (Fig. 3). The lowermost investigated sample (31.17 m) is assigned to the uppermost Pliensbachian NJT 5 Zone (NJT 5b Subzone) based on the presence of *L. hauffii* and *L. sigillatus*. The NJT 5/NJT 6 zonal boundary is correlatable with the base of the Fish Level, although we precise that the FO of *C. superbus crassus* was observed 0.8 cm above the base of the lowermost black shale (26.932 m) (Fig. 3). The FO of *D. ignotus* is placed at 26.938 m, in the topmost NJ 5b Subzone.

Within the basal part of the NJT 6 Zone the FOs of rare and discontinuous *C. poulnabronei*, *L. crucicentralis, L. velatus* and *D. constans* were detected within a 4.8 cm thick interval. These findings suggest a hiatus at the base of the black shale interval of the Fish Level eliding part of the latest Pliensbachian-early Toarcian time interval.

In the NJT 6 Zone, the LO of *M. jansae* (13.74 m) was detected and used to identify the base of the NJT 6b Subzone of Ferreira et al. (2019) (Fig. 3). The uppermost investigated sample (3.08 m) is still included in the early Toarcian NJT 6 Zone due to the absence of *D. striatus*, which is the zonal marker of the base of the NJT 7 Zone (Mattioli & Erba 1999).

The *Schizosphaerella* decline was not observed in the Gajum Core, further indicating the absence of the Domaro Lmst./Sogno Fm. boundary interval. The *Schizosphaerella* and *M. jansae* crises were detected at the base of the Fish Level (26.94 m). However, as explained above, the lithostratigraphic boundary between the Domaro Lmst. and the Sogno Fm. is marked by a hiatus and, consequently, the *Schizosphaerella* and *M. jansae* crises are presumably apparent and not real events in the Gajum Core. The *Schizosphaerella* recovery was detected at 12.89 m in the upper part of the Fish Level where this genus become continuous and rare to frequent.

The calcareous nannofossil assemblages of the NJT 5b Subzone are dominated by *S. punctulata* and *M. jansae*. Among schizosphaerellids, *S. punctulata* and "small" *S. punctulata* are the most abundant morphotypes (rare/frequent to common/abundant and rare/frequent to common, respectively) whereas "encrusted" *S. punctulata* is subordinated (rare to frequent/common). Within the genus *Mitrolithus, M. jansae* is relatively more abundant (rare to frequent) than "thin" *M. jansae* (extremely rare to rare/frequent) (see range chart in Appendix 3).

Nannofossil assemblages of the NJT 6a Subzone corresponding to the Fish Level show a drastic reduction in abundance of both *Schizosphaerella* and *Mitrolithus* (*Schizosphaerella* and *M. jansae* crises). In particular, both *S. punctulata* and "small" *S. punctulata* become rare whereas "encrusted" *S. punctulata* is extremely sparse, although in some samples schizosphaerellids displays a frequent/common abundance. Similarly to the Sogno Core, within the Fish Level *M. jansae* is equally represented by both normal and thin morphotypes becoming discontinuous and generally rare. In the Fish Level *Lotharingius* is the dominant genus with *L. hauffii* as most abundant species.

PLATE 2

Scale bars represent 2 μm.

1-2 - *L. frodoi*, 1) cross-polarized light, 2) quartz lamina, Gajum Core, sample G C22 854 (23.39 m)
3-4 - *L. hauffii*, 3) cross-polarized light, 4) quartz lamina, Gajum Core, sample G C6 221 (8.14 m)
5-6 - *L. sigillatus*, 5) cross-polarized light, 6) quartz lamina, Gajum Core, sample G C20 810 (22.19 m)
7-8 - *L. umbriensis*, 7) cross-polarized light, 8) quartz lamina, Gajum Core, sample G C7 275 (9. 15 m)
9-10 - *L. velatus*, 9) cross-polarized light, 10) quartz lamina, Gajum Core, sample G C5 160 (6.84 m)
11-12 - *M. elegans*, 11) cross-polarized light, 12) quartz lamina, Sogno Core, sample S3 C30 466 (26.2 m)
13-14 - *M. jansae*, 13) cross-polarized light, 14) quartz lamina, Gajum Core, sample G C25 995 (26.94 m)
15-16 - "thin" *M. jansae*, 15) cross-polarized light, 16) quartz lamina, Sogno Core, sample S3 C24 441 (24.38 m)
17-18 - "thin" *M. jansae*, 17) cross-polarized light, 18) quartz lamina, Gajum Core, sample G C25 993 (26.87 m)
19-20 - *M. lenticularis*, 19) cross-polarized light, 20) quartz lamina, Sogno Core, sample S3 C12 330 (17.16 m)
21-22 - *S. cruciulus,* 21) cross-polarized light, 22) quartz lamina, Gajum Core, sample G C25 995 (26.94 m)
23-24 - *S. punctulata,* 23) cross-polarized light, 24) quartz lamina, Sogno Core, sample S3 C20 409 (22.5 m)
25-26 - *S. punctulata,* 25) cross-polarized light, 26) quartz lamina, Gajum Core, sample G C15 599 (16.55 m)
27-28 - "small" *S. punctulata,* 27) cross-polarized light, 28) quartz lamina, Sogno Core, sample sample S3 C24 439 (24.22 m)
29-30 - "encrusted" *S. punctulata,* 29) cross-polarized light, 30) quartz lamina, Sogno Core, sample S3 C20 401 (22 m)
31-32 - *T. patulus,* 31) cross-polarized light, 32) quartz lamina, Sogno Core, sample S3 C13 335 (17.45 m)
33-34 - *Watznaueria* sp.1, 33) cross-polarized light, 34) quartz lamina, Sogno Core, sample S1 C24 164 (10.47 m)

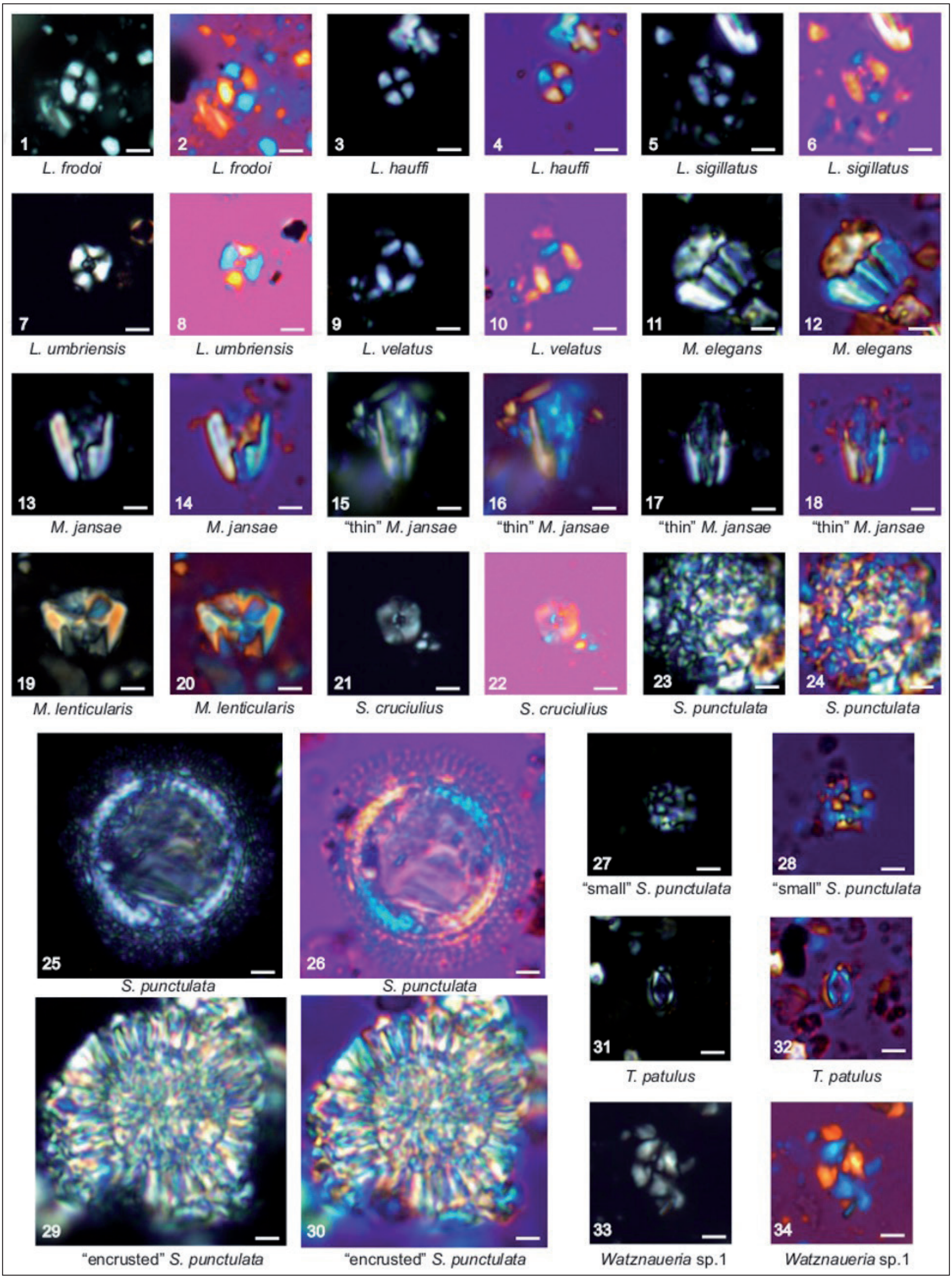

L. frodoi *L. frodoi* *L. hauffi* *L. hauffi* *L. sigillatus* *L. sigillatus*

L. umbriensis *L. umbriensis* *L. velatus* *L. velatus* *M. elegans* *M. elegans*

M. jansae *M. jansae* "thin" *M. jansae* "thin" *M. jansae* "thin" *M. jansae* "thin" *M. jansae*

M. lenticularis *M. lenticularis* *S. cruciulius* *S. cruciulius* *S. punctulata* *S. punctulata*

S. punctulata *S. punctulata* "small" *S. punctulata* "small" *S. punctulata*

T. patulus *T. patulus*

"encrusted" *S. punctulata* "encrusted" *S. punctulata* *Watznaueria* sp.1 *Watznaueria* sp.1

Plate 2

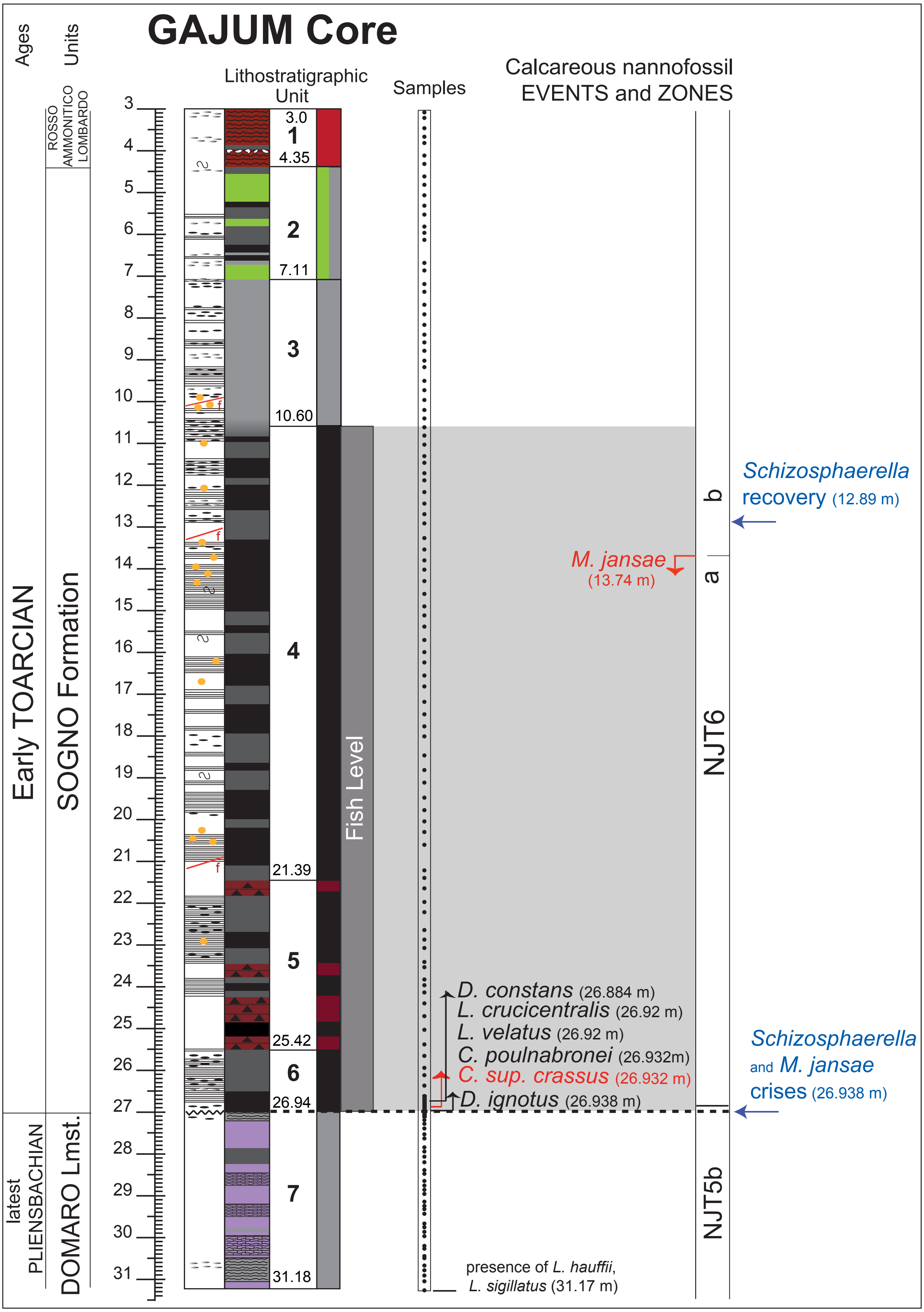

Fig. 3 - Lithostratigraphy and biostratigraphy of the Gajum Core. Calcareous nannofossil events in red are the primary events used as zonal and subzonal boundaries. The *Schizosphaerella* and *M. jansae* crises, and the *Schizosphaerella* recovery are reported in blue. Legend as in Figure 2.

In the uppermost part of the Fish Level, calcareous nannofossil assemblages are characterized by a general recovery in abundance of schizosphaerellids (*Schizosphaerella* recovery). However, only *S. punctulata* and "small" *S. punctulata* were observed (extremely rare to frequent/common) whereas "encrusted" *S. punctulata* disappears. In the uppermost studied interval represented by the Rosso Ammonitico Lombardo Fm., the family Calyculaceae shows an increase in abundance of both *Calyculus* and *Carinolithus*, passing from extremely rare to frequent.

Through the Gajum Core, genera *Biscutum* and *Crepidolithus* are characterized by rare abundance, whereas *Bussonius*, *Diductius*, *Similiscutum, Parhabdolithus* and *Tubirhabdus* are extremely rare.

DISCUSSION

Correlation of the Sogno Core to the Colle di Sogno section.

Before coring, the section outcropping at Colle di Sogno was studied for calcareous nannofossil biostratigraphy and paleoceanography by Erba (2004), Channell et al. (2010) and Casellato & Erba (2015). The stratigraphic interval studied in detail by Casellato & Erba (2015) spans from the upper Pliensbachian (Domaro Lmst.) to the lower Toarcian (Sogno Fm.) and is comparable, but not identical, to the Sogno Core succession. In fact, the Sogno Core terminated at a stratigraphic level younger than the Colle di Sogno outcrop section and, therefore, some nannofossil events were not detected in the present work (FOs of *Calyculus* spp., *Biscutum grande*, *Bussonius prinsii*, *Lotharingius frodoi* and *Bussonius leufuensis*). Conversely, the upper 5 meters of the Sogno Core are younger than the top of the Colle di Sogno section (Casellato & Erba 2015).

As expected, the stratigraphic levels of FOs and LOs found in the Sogno Core are fully consistent with data documented for the Colle di Sogno section by Casellato & Erba (2015). This is the case for the FOs of *C. poulnabronei*, *L. crucicentralis, Watznaueria* sp. 1, the LO of *M. jansae,* the *Schizosphaerella* decline, crisis, recovery, and the *M. jansae* crisis. Only a few events, such as the FOs of *L. sigillatus*, *D. constans* and *C. superbus crassus,* were detected at slightly lower stratigraphic levels in the Sogno Core relative to the Colle di Sogno outcrop. Relatively higher incongruities regarding the FOs of *L. velatus* and *D. ignotus* were detected below the Fish Level in the Sogno Core but within the Fish Level in the Colle di Sogno section. Such stratigraphic differences are, presumably, attributable to a better preservation and higher sampling rates of the Sogno Core, concurring to improved detection of rare taxa. In fact, observed discrepancies mostly depend on the discontinuous range of taxa in their initial ranges (see range chart in Appendix 2). Moreover, the generally better preservation state of the cored material increases the possibility of finding the most delicate taxa.

Due to their scantiness, the LOs of *S. cruciulus* and *M. lenticularis* were only tentatively placed in the Sogno Core in the upper part of the Fish Level and above the FO of *Watznaueria* sp. 1, respectively, at stratigraphic levels comparable to those documented in the Colle di Sogno section (Casellato & Erba 2015).

As far as the LO of the standard morphotype of *M. jansae* is concerned, it was placed at the base of the Fish Level in the Colle di Sogno outcrop, based on absolute abundances obtained in thin sections (Casellato & Erba 2015: Fig. 8). This datum was named Last Common Occurrence (LCO) of *M. jansae* and was correlated to similar events at supra-regional scale (Casellato & Erba 2015). However, sparse specimens of *M. jansae* were documented within the Fish Level outcropping at Colle di Sogno (Casellato & Erba 2015), consistently with data obtained for the Sogno Core (this study). The two morphotypes of *M. jansae* co-occur in the Fish Level, although rare and discontinuous, and the LO of this species was located above the top of the black shale interval both in the outcrop and in the Sogno Core.

Correlation of the Sogno and Gajum Cores

Calcareous nannofossil preservation, abundance, and biostratigraphy display quite consistent results between the two investigated core successions. The stratigraphic interval spans from the upper Pliensbachian (Domaro Lmst.) to the lower Toarcian (Sogno Fm./Rosso Ammonitico Lombardo Fm.), including the lithological expression of the T-OAE (Fish Level) in both cores (Fig. 4). The biostratigraphic results indicate that the Sogno Core recovered a slightly longer interval as documented by the FOs of *L. sigillatus* in the lowermost part and *Watznaueria* sp.1 in the upper part of the Sogno Core.

According to their geological settings, the successions recovered in the Sogno and Gajum Cores are characterized by a continuous and incomplete record, respectively (Fig. 4). In fact, the FOs of *C. poulnabronei*, *L. crucicentralis*, *L. velatus* and *D. ignotus* were detected at different stratigraphic levels in the Sogno Core, but in a few cm thick interval in the lowermost part of the Fish Level of the Gajum Core, revealing the presence of a hiatus. This is further evidenced by the absence of the *Schizosphaerella* decline and the occurrence of the *Schizosphaerella* and *M. jansae* crises in correspondence of the base of the black shale interval. Figure 4 illustrates the biostratigraphic correlations of the two cored sequences, providing the estimate of the interval missing in the Gajum Core. Calcareous nannofossil events, however, suggest that the onset of the Fish Level is most probably preserved. Conversely, the lowermost Toarcian (and possibly the topmost Pliensbachian) is not recorded in the Gajum Core due to the first co-occurrence of *D. ignotus, C. poulnabronei*, *L. crucicentralis*, *L. velatus* and in the basal part of the Fish Level. Indeed, the Domaro Lmst. is immediately overlain by black shales of the Fish Level, while in pelagic complete sections, as for instance the Sogno Core (Erba et al. 2019b) and the Colle di Sogno section (Gaetani & Poliani 1978; Casellato & Erba 2015), the Fish Level is preceded by the lowermost part of the Sogno Fm. We estimate that ~ 600kys are missing adopting the zonal scheme of Mattioli & Erba (1999) and the Time Scale of Gradstein et al. (2012) (Fig. 5). The detection of a hiatus in the lower Toarcian before the T-OAE black shales is a rather common feature in Western Tethyan areas (Wignall 1991; Morard et al. 2003; Röhl & Schmid-Röhl 2005; Léonide et al. 2012; Mattioli et al. 2013; Pittet et al. 2014; Menini et al. 2019; Visentin et al. 2021b).

The FO of *C. superbus crassus* shows relatively consistent results between the two cores although this biohorizon was detected at a slightly higher stratigraphic level in the Gajum Core (within the basal part of the Fish Level). This minor difference is possibly imputed to the scarcity of this taxon in its initial range or might suggest an earlier onset of anoxic sedimentation at Gajum.

The *Schizosphaerella* and *M. jansae* crises were detected at the base of the Fish Level in both the Sogno and Gajum Cores, although in the latter core this event is presumably apparent (see discussion above). Schizosphaerellid abundances are different in the two studied successions: reflecting the relatively higher carbonate content in a few levels of the Gajum Fish Level, abundances of schizosphaerellids vary from absent to common/abundant. The *Schizosphaerella* recovery and the LO of *M. jansae* (both standard and thin morphotypes) display very consistent results in the two cored successions.

Comparison with the Tethyan nannofossil zonation

The zonal scheme of Mattioli & Erba (1999) proposed as reference for Tethyan and lower latitude sections and, more specifically, for the Mediterranean province, is used to discuss the nannofossil biohorizons detected in this work (Fig. 5). After 20 years of nannofossil biostratigraphic investigations of Lower Jurassic sections the events and zones proposed by Mattioli & Erba (1999) have been tested and partly revised (see Ferreira et al. 2019 for a synthesis). It must be emphasized that the fundamental structure – consisting in marker events and derived biozones - remains, however, confirmed.

The nannofossil zonal biohorizons recognized in the Sogno and Gajum Cores are fully consistent with the scheme of Mattioli & Erba (1999) as discussed below, from bottom to top:

* the FO of *L. sigillatus* defining the base of the NJT 5b Subzone was detected in the uppermost Pliensbachian Domaro Lmst. in both cores. As discussed by Casellato & Erba (2015), the original use of this event to define the Pliensbachian/Toarcian boundary has been revised to a slightly older age within the latest Pliensbachian (see also discussion in Ferreira et al. 2019);

* the FO of *C. superbus crassus* used to determine the base of the NJT 6 Zone was found at the onset of the T-OAE black shale interval in both cores. We specify here that, according to Visentin et al. (2021a), *C. superbus crassus* corresponds to *C. superbus* of Mattioli & Erba (1999);

* the LO of *M. jansae* was detected above and in the uppermost part of the Fish Level black shales in the Sogno and Gajum Cores, respectively. Although originally this biohorizon was proposed by Mattioli & Erba (1999) as a secondary event to be

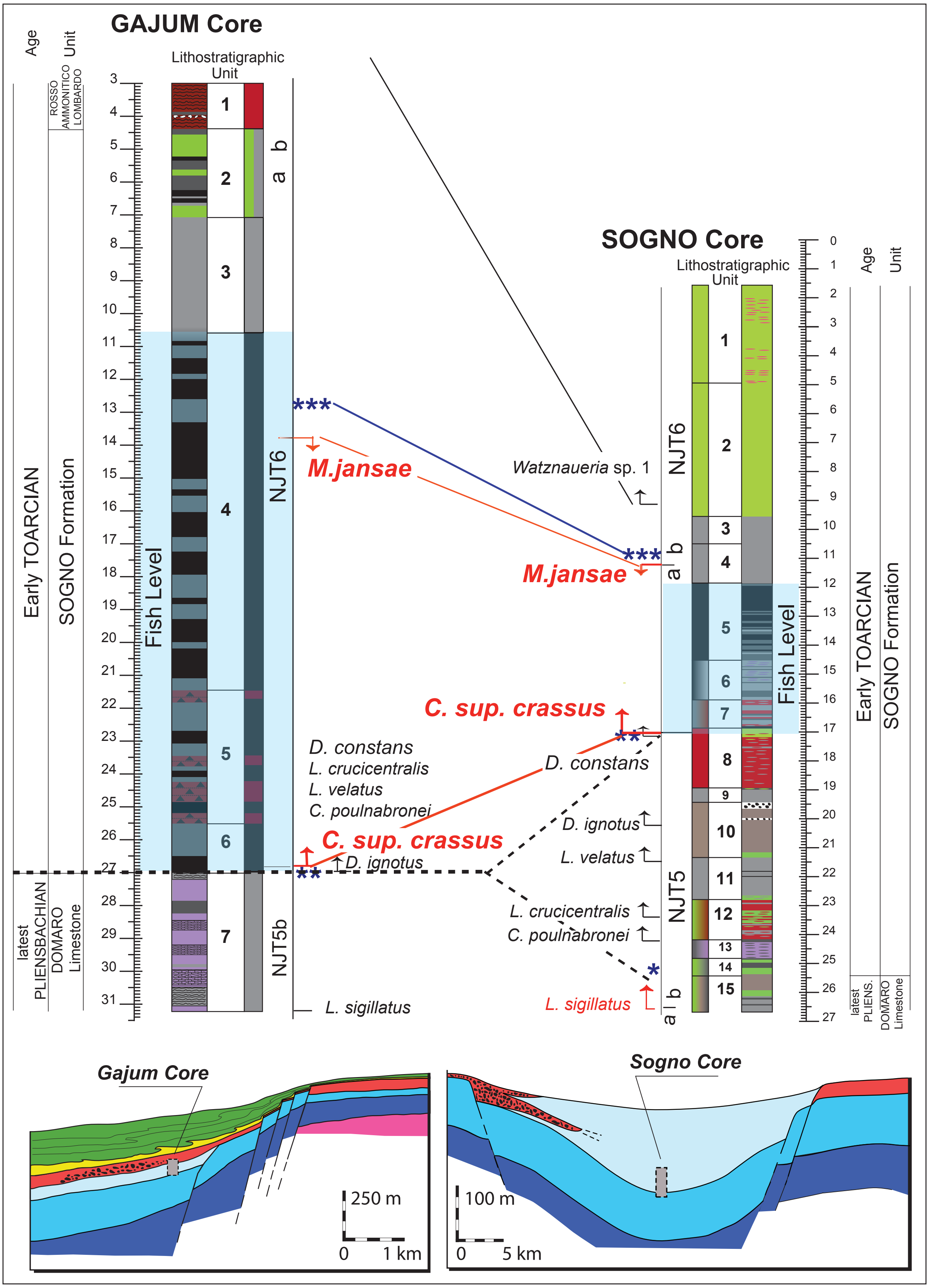

Fig. 4 - Calcareous nannofossil biostratigraphic correlation of the Sogno and Gajum Cores showing that the lowermost Toarcian Sogno Fm. is missing at Gajum. In the lower part of the figure, the Sogno and Gajum Cores are contestualised on the Albenza Plateau and on the flank of the Corni di Canzo High (after Erba et al. 2019b).

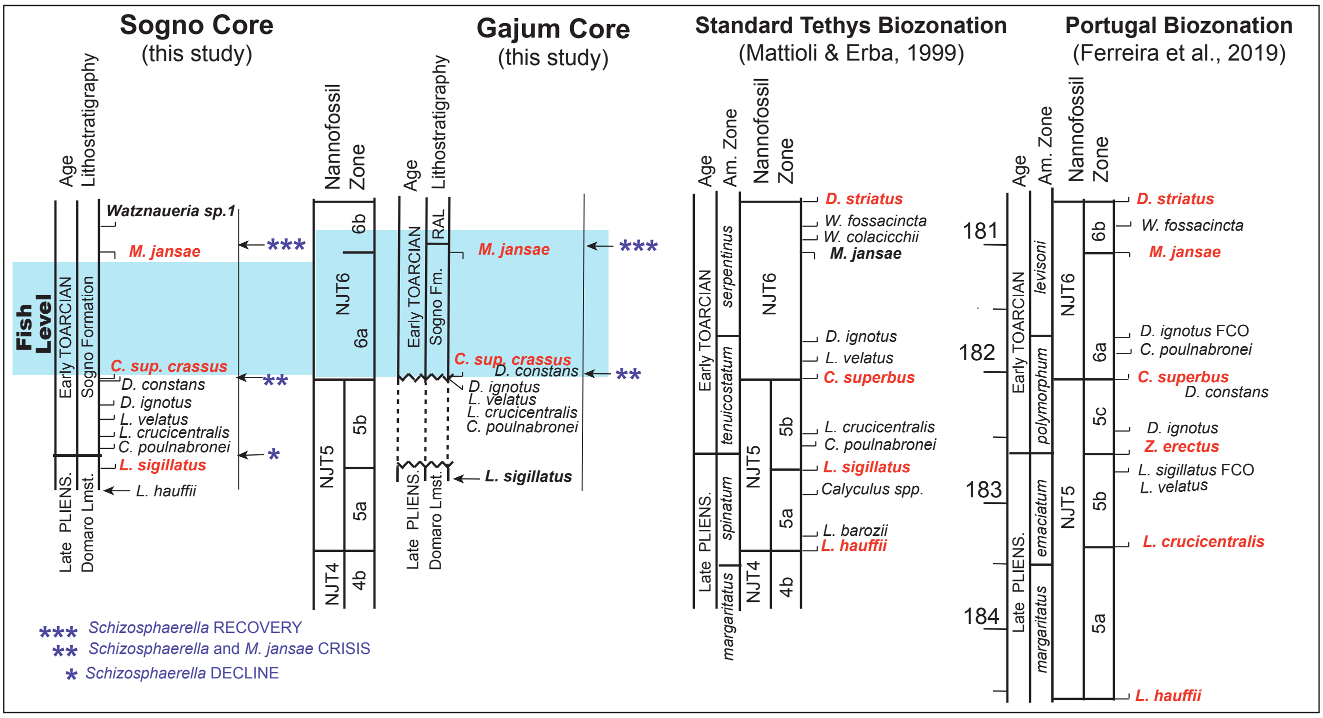

Fig. 5 - Comparison of the results obtained for the Sogno and Gajum Cores with the zonations of Mattioli & Erba (1999) and Ferreira et al. (2019). Zonal and subzonal events are reported in red.

confirmed, its reproducibility makes this datum fully reliable at low latitudes (Casellato & Erba 2015) and we use it to separate the NJT 6 Zone into 2 subzones as suggested by Ferreira et al. (2019).

The zonal scheme recently proposed by Ferreira et al. (2019) for the Lusitanian Basin is also considered here (Fig. 5). Events, zones, and subzones are based on detailed investigation of several Lusitanian successions, including two GSSP sections, located during the Jurassic in the Western Tethys and, thus, acting as a north-south migration pathway for several organisms, including calcareous nannoplankton and ammonites. Ferreira et al. (2019) calibrated nannofossil biohorizons against Ammonite Zones (AZs) as well as against carbon and oxygen isotope excursions where possible. Moreover, the work by Ferreira et al. (2019) includes an updated and revised taxonomy and a comprehensive synthesis of biostratigraphies from the Western Tethys.

As far as the marker events are concerned, the FO of *C. superbus crassus* (= *C. superbus* in Ferreira et al. 2019) and LO of *M. jansae* are comparable with our findings and the zonation of Mattioli & Erba (1999) (Fig. 5). Conversely, Ferreira et al. (2019) placed the FO of *L. sigillatus* within the NJT 4 Zone (base of their NJT 4e Subzone) of late Pliensbachian age (Margaritatus AZ), thus, at a definitively older stratigraphic level relative to Mattioli & Erba (1999) and our data from the Sogno and Gajum Cores. Ferreira et al. (2019) stated that the earliest specimens of *L. sigillatus* recorded in the upper Pliensbachian of the Rabaçal section are significantly smaller (average distal shield diameter of 4.34 µm; Ferreira et al. 2017) than the size range provided in the original description by Stradner (1961) (6-8 µm). Nevertheless, since these early specimens show identical diagnostic features and their sizes are not very different from those documented in the emendation by Goy (1981), Ferreira et al. (2019) considered them within *L. sigillatus*. We notice that Ferreira et al. (2019) report the first common occurrence (FCO) of *L. sigillatus* at the stratigraphic level of the FO of *L. sigillatus* of Mattioli & Erba (1999) and as found in the Sogno and Gajum Cores (Fig. 5).

The FO of *L. crucicentralis* is also older in the zonal scheme of Ferreira et al. (2019), who placed this event within the lowermost Emaciatum AZ at the base of the NJT 5b Subzone (late Pliensbachian). These authors specified that several specimens of *L. crucicentralis*, although with diagnostic features matching those described by Medd (1971) and emended by Grün & Zweili (1980), are significantly smaller in size. In this study, we adopted taxonomic features of *L. sigillatus* and *L. crucicentralis* consistent with those of Ferreira et al. (2019), without using differentiation based on coccolith size. Therefore, we conclude that the FOs of *L. sigillatus* and *L. crucicentralis* are diachronous, being older in the Lusitanian Basin relative to the Mediterranean province in the Tethys Ocean.

Among the secondary events, the FO of *C. poulnabronei* detetcted in the Sogno Core is consistent exclusively with that of Mattioli & Erba (1999). Ferreira et al. (2019), indeed, placed this event within the uppermost Polymorphum AZ, just after the FO of *C. superbus crassus*. It is possible, however, that this discrepancy is mainly the result of the discontinuous occurrence of this taxon in its initial range rather than diachroneity. The FO of *C. poulnabronei*, indeed, was reported by Ferreira et al. (2019) only in the Peniche section and looking at the range charts provided in the supplementary material *C. poulnabronei* occurs sporadically, thus not excluding a potentially older first occurrence. Conversely, the FO of *D. ignotus* detected in our study shows consistency with the biozonation of Ferreira et al. (2019), while Mattioli & Erba (1999) assigned a younger age to this event, between the FOs of *C. superbus crassus* and the LO of *M. jansae*. The reason of this discrepancy is also probably attributable to scantiness of this taxon. In fact, according to Mattioli et al. (2013), *D. ignotus* has a Lazarus behaviour, first occurring in the earliest Toarcian, being absent from the sediments corresponding to the T-OAE and subsequently occurring consistently from the end of the T-OAE upwards. This distribution was observed not only at Peniche, but also in sections of the Mediterranean province, namely, Valdorbia in central Italy (Mattioli et al. 2013), Amellago in Marocco (Bodin et al. 2010) and La Almunia in South-Eastern Spain (Menini et al. 2019). Although our findings confirm that the FO of *D. ignotus* precedes the onset of the T-OAE black shales within the NJT 5b Subzone of Mattioli & Erba (1999), it is possibly coeval with the datum of Ferreira et al. (2019) within their NJT 5c Subzone. The stratigraphic level of the FO of *D. ignotus* of the Mattioli & Erba (1999) zonation appears to be equivalent to the FCO of this taxon in the zonal scheme of Ferreira et al. (2019) (Fig. 5).

As far as the FO of *L. velatus* is concerned, our finding is inconsistent with the zonal schemes of Ferreira et al. (2019) and Mattioli & Erba (1999) who proposed an older (shortly before the FO of *Z. erectus*) and younger (between the FOs of *C. superbus crassus* and *D. ignotus*) age, respectively. The FO of *D. constans* was not considered in Mattioli & Erba (1999), and our results fit well with the datum proposed by Ferreira et al. (2019).

In our study, the FO of *Watznaueria* sp. 1 corresponds to the FO of *W. fossacincta* in both the zonations by Mattioli & Erba (1999) and Ferreira et al. (2019). The taxonomic characterization of *Watznaueria* sp. 1 described by Cobianchi (1992) and Casellato & Erba (2015) are applied here.

Differently from the biozonation of Mattioli & Erba (1999), the FO of *W. colacicchii*, reported between the LO of *M. jansae* and the FO of *Watznaueria* sp. 1 (= *W. fossacincta*), was not found in the Sogno and Gajum Cores as this taxon is absent in the investigated interval. Also Casellato & Erba (2015) did not observe *W. colacicchii* in the Colle di Sogno section. Ferreira et al. (2019) place the FO of *W. colacicchii* in the lower part of the NJT 7 Zone at the base of the Bifrons AZ, thus at a stratigraphic level younger than the zonation of Mattioli & Erba (1999) and the interval here investigated.

Nannofossil events reported by Ferreira et al. (2019), but not by Mattioli & Erba (1999), and not identified in the Sogno and Gajum Cores are, from the oldest to youngest, the FOs of *Axopodorhabdus atavus*, *Zeugrhabdotus erectus*, *Ethmorhabdus* spp. and LO of *Mazaganella protensa*. This major difference is presumably linked to nannoplankton provincialism during the Early Jurassic which further supports the necessity of two biozonation schemes applicable in the Lusitanian Basin and the Mediterranean Province, respectively.

SUMMARY AND CONCLUSIONS

High-resolution calcareous nannofossil biostratigraphy carried out in two cores drilled in the Lombardy Basin allowed the identification of nine (Sogno Core) and seven (Gajum Core) events in the uppermost Pliensbachian Domaro Lmst. and the lower Toarcian Sogno Fm. and Rosso Ammonitico Lombardo Fm. As expected, relative to the Colle di Sogno outcrop calcareous nannofossils are better preserved in the Sogno Core and the high-resolution sampling resulted in improved detection of events. The correlation of the Sogno and Gajum nannofossil biostratigraphy shows that, according to their geological settings, the succession recovered in the

Sogno Core (located on the Albenza Plateau) is continuous while a hiatus of ~600 kyrs was detected at the base of the Fish Level in the Gajum Core. However, nannofossil data suggest that the black shale interval is complete whereas the lowermost Toarcian basal portion of the Sogno Fm. (and possibly the topmost Pliensbachian Domaro Lmst.) is missing in the Gajum Core.

Following the standard nannofossil zonation for the Mediterranean Province in the Tethys Ocean (Mattioli & Erba 1999), the NJT 5 and NJT 6 Zones were identified in both the Sogno and Gajum Cores. Furthermore, as proposed by Ferreira et al. (2019), we adopt the LO of *M. jansae* to separate the NJT 6a and NJT 6b Subzones. In the Sogno and Gajum Cores, the Fish Level, regionally considered the lithological expression of the T-OAE, results to be largely constrained between the FO of C. *superbus crassus* and the LO of *M. jansae* (NJT 6a Subzone), although black shales continue for a short interval above the LO of *M. jansae* in the Gajum Core. Therefore, nannofossil biostratigraphy suggest that anoxic conditions did not cease simultaneously in nearby sites within the Lombardy Basin.

Other nannofossil events useful for the biostratigraphic characterization of the T-OAE are the FO of *D. constans* and the *Schizosphaerella* - *M. jansae* crises at the base of the Fish Level and the *Schizosphaerella* recovery following the LO of *M. jansae*.

The comparison between the results of our investigation and the zonal schemes established for the Tethys Ocean (Mattioli & Erba 1999; Ferreira et al. 2019) revealed consistencies and differences. Confirming the Mediterranean affinity of the studied sites, calcareous nannofossil biohorizons identified in the Sogno and Gajum Cores are mostly coherent with the biozonation of Mattioli & Erba (1999), that is, however, here improved separating the NJT 6 Zone into two subzones.

The zonation of Ferreira et al. (2019) established for the Western Tethys Lusitanian Basin is only partially reproducible, in practice only for the NJT 6 zonal markers, thus confirming the supra-regional value of the FO of *C. superbus crassus* and the LO of *M. jansae*. Another event traceable from the Mediterranean area to the Lusitanian Basin is the FO of *Watznaueria* sp. 1 in the NJT 6b Subzone.

Some discrepancies might be explained by the abundance/rarity of taxa in different areas. In fact, Ferreira et al. (2019) report the FCO of *L. sigillatus* at the stratigraphic level of the FO of *L. sigillatus* of Mattioli & Erba (1999) and as found in the Sogno and Gajum Cores. Similarly, we detected the FO of *D. ignotus* within the NJT5b Subzone of Mattioli & Erba (1999) at a stratigraphic level comparable to that of Ferreira et al. (2019), but definitively before the datum of the Mattioli & Erba (1999) whose FO of *D. ignotus* appears to be equivalent to the FCO of this taxon in the zonal scheme of Ferreira et al. (2019). Contrarily to Mattioli & Erba (1999), we did not observe *W. colacicchii* in the NTJ 6b Subzone as in the zonation of Ferreira et al. (2019), who report the FO of *W. colacicchii* in the lower part of the NJT 7 Zone at the base of the Bifrons AZ, thus at a stratigraphic level younger than the investigated interval.

Our finding of the FO of *L. velatus* is inconsistent with the zonal scheme of Ferreira et al. (2019) while Mattioli & Erba (1999) proposed a younger age between the FOs of *C. superbus crassus* and *D. ignotus*. This disparity along with the absence of several marker species used in the zonation of Ferreira et al. (2019) support the existence of a prominent nannoplankton provincialism between Portugal and the Mediterranean Province during the Early Jurassic and, therefore, justify the use of partially different zonal schemes. We underline, however, that at supra-regional scale the T-OAE is unambiguously constrained by the FO of *C. superbus crassus* and the LO of *M. jansae*.

Acknowledgments: The Associate Editor Isabella Raffi, the Reviewers Angela Fraguas and Emanuela Mattioli are warmly acknowledged for their constructive detailed criticism that much improved the quality of the manuscript. The T-OAE coring project in the Lombardy Basin derived from fieldwork and stratigraphic characterization of Jurassic successions with Maurizio Gaetani. The Sogno and Gajum coring campaign was funded by MIUR-PRIN2011(2010X3PP8J) awarded to EE., while the nannofossil biostratigraphic characterization was conducted within the PRIN 2017RX9XXXY awarded to EE.

REFERENCES

Bernoulli D. & Jenkyns H. C. (2009) - Ancient oceans and continental margins of the Alpine-Mediterranean Tethys: Deciphering clues from Mesozoic pelagic sediments and ophiolites. *Sedimentology* 56(1): 149–190.

Bodin S., Mattioli E., Fröhlich S., Marshall J.D., Boutib L., Lahsini S. & Redfern J. (2010) - Toarcian carbone isotope shifts and nutrient changes from the Northen margin of Gondwana (High Atlas, Morocco, Jurassic): Palaeonviromental implications. *Palaeogeography, Palaeoclimatology, Palaeoecology,* 297: 377-390.

Bown P. R. (1987) - Taxonomy, evolution, and biostratigraphy of Late Triassic-Early Jurassic calcareous nannofossils. *Palaeontological Association, Special papers on Palaeontology,* 32: 1-118.

Bown P.R. & Cooper M.K.E. (1998) - Jurassic. In: Bown P.R. (Ed.) - Calcareous nannofossil biostratigraphy. *British Micropaleontological Society Published Series*: 34-85. Kluwer Academic Publishers, London.

Bown P.R., Lees J.A. & Young J.R. (2004) - Calcareous nannoplankton evolution and diversity through time. In: Thierstein H.R. & Young J.R. (Eds) - Coccolithophores: from molecular processes to global impact: 481-508. Springer, Berlin, Heidelberg.

Casellato C.E. & Erba E. (2015) - Calcareous nannofossil biostratigraphy and paleoceanography of the Toarcian Oceanic Anoxic event at Colle di Sogno (Southern Alps, Northern Italy). *Rivista Italiana di Paleontologia e Stratigrafia,* 121(3): 297-327.

Channell J.E.T., Casellato C.E., Muttoni G. & Erba E. (2010) - Magnetostratigraphy, nannofossil stratigraphy and apparent polar wander for Adria-Africa in the Jurassic - Cretaceous boundary interval, *Palaeogeography, Palaeoclimatology, Palaeoecology*, 293(1-2): 51-75.

Clémence M.E., Gardin S. & Bartolini A. (2015) - New insights in the pattern and timing of the Early Jurassic calcareous nannofossil crisis. *Palaeogeography, Palaeoclimatology, Palaeoecology*, 427: 100-108.

Cobianchi M. (1992) - Sinemurian - Early Bajocian calcareous nannofossil biostratigraphy of the Lombardian Basin (Southern calcareous Alps; Northern Italy). *Atti Ticinensi di Scienze della Terra*, 35: 61-106.

Erba E. (2004) - Calcareous nannofossils and Mesozoic oceanic anoxic events. *Marine Micropaleontology*, 52: 85-106.

Erba E. (2006) - The first 150 million years history of calcareous nannoplankton: Biosphere - Geosphere interactions. *Palaeogeography, Palaeoclimatology, Palaeoecology*, 232: 237-250.

Erba E. & Casellato C.E. (2010) - Paleoceanografia del Giurassico nella Tetide occidentale: l'archivio geologico del Bacino Lombardo. *Rendiconti dell'Istituto Lombardo, Accademia di Scienze e Lettere, Special Publication on "Una nuova Geologia per la Lombardia"*, 447: 115-140.

Erba E., Bottini C., Faucher G., Gambacorta G. & Visentin S. (2019a) - The response of calcareous nannoplankton to Oceanic Anoxic Events: the Italian pelagic record. *Bollettino della Società Paleontologica Italiana,* 58(1): 51-71.

Erba E., Gambacorta G., Visentin S., Chavalheiro L., Reolon D., Faucher G. & Pegoraro M. (2019b) - Coring the sedimentary expression of the Early Toarcian Oceanic Anoxic Event: new stratigraphic records from the Tethys Ocean. *Scientific Drilling*, 7: 1-12.

Ferreira J., Mattioli E. & Van de Schootbrugge B. (2017) - Palaeoenvironmental vs. evolutionary control on size variation of coccoliths across the Lower-Middle Jurassic. *Palaeogeography, Palaeoclimatology, Palaeoecology*, 465: 177-192.

Ferreira J., Mattioli E., Sucheràs-Marx B., Giraud F., Duarte V. L., Pittet B., Suan G., Hassler A. & Spangenberg J.E. (2019) - Western Tethys Early and Middle Jurassic calcareous nannofossil biostratigraphy. *Earth-Science Reviews,* 197: 1-19.

Fraguas A. & Young J.R. (2011) - Evolution of the coccolith genus *Lotharingius* during the Late Pliensbachian-Early Toarcian interval in Asturias (N Spain). Consequences of the Early Toarcian environmental perturbations. *Geobios*, 44: 361-375.

Fraguas A., Comas-Rengifo M.J., Gomez J.J. & Goy A. (2012) - The calcareous nannofossil crisis in Northen Spain (Asturias province) linked to the Early Toarcian warming-driven mass extinction. *Marine Micropalentology*, 94-95: 58-71.

Fraguas A., Comas-Rengifo M.J. & Perilli N. (2015) - Calcareous nannofossil biostratigraphy of the Lower Jurassic in the Cantabrian Range (Northen Spain). *Newsletter on Stratigraphy*, 48(2): 179-199.

Fraguas A., Comas-Rengifo M.J., Goy A. & Gómez J.J. (2018) - Upper Sinemurian–Pliensbachian calcareous nannofossil biostratigraphy of the E Rodiles section (Asturias, N Spain): a reference section for the connection between the Boreal and Tethyan Realms. *Newsletters on Stratigraphy,* 51/2: 227-244.

Gaetani M. (1975) - Jurassic stratigraphy of the Southern Alps: a review. *Geology of Italy*, 1: 377-402.

Gaetani M. (2010) - From Permian to Cretaceous: Adria as pivotal between extensions and rotations of Tethys and Atlantic Oceans. In: Beltrando M., Peccerillo A., Mattei M., Conticelli S. & Doglioni C. (Eds) - Geology of Italy. *Journal of the Virtual Explorer*, 36: 5.a.

Gaetani M. & Poliani G. (1978) - Il Toarciano e il Giurassico medio in Albenza (Bergamo). *Rivista Italiana di Paleontologia e Stratigrafia,* 84(2): 349-382.

Gaetani M. & Erba E. (1990) - Il Bacino Lombardo: un sistema paleoalto/fossa in un margine continentale passivo durante il Giurassico. 75° Congresso Società Geologica Italiana. Guida alle escursioni precongresso. Escursione A3.

Geisen M., Bollmann J., Herrle J.O., Mutterlose J. & Youg J. R. (1999) - Calibration of the random settling technique for calculation of absolute abundances of calcareous nannoplankton. *Micropaleontology,* 45: 437-442.

Goy G. (1981) - Nannofossiles calcaires des schistes carbon (Toarcien Inferieur) du Bassin de Paris. Doc. de la RCP 459. *Nature et genèse des facies confinés*, editions du BRGM: 1-86.

Gradstein F.M., Ogg J.G., Schmitz M.B. & Ogg G.M. (2012) - The geologic time scale 2012. Elsevier, 2012.

Grün W. & Zweili F. (1980) - Das kalkige Nannoplankton der Dogger-Malm-Grenze im Berner Jura bei Liesberg (Schweiz). *Neues Jahrbuch für Geologie und Paläontologie Abhandlungen*, 123(1): 231-341.

Hesselbo S.H., Gröcke D.R., Jenkyns H.C., Bjerrun C.J., Farrimond P., Morgans Bell H.S. & Green O.R. (2000) - Massive dissociation of gas hydrate during a Jurassic oceanic anoxic event. *Nature*, 406: 392-395.

Hinnov L.A., Park J. & Erba E. (2000) - Lower-Middle Jurassic rhythmites from the Lombard Basin, Italy: a record of orbitally forced carbonate cycles modulated by secular environmental changes in West Tethys. In: Hall R.L. &

Smith P. L. (Eds) - Advances in Jurassic Research 2000. *GeoResearch Forum*, 6: 427-436. Trans Tech Publications Zurich, Switzerland.

Jenkyns H.C. (1985) - The Early Toarcian and Cenomanian-Turonian anoxic events in Europe: comparisons and contrasts. *Geologische Rundschau,* 74(3): 505-518.

Jenkyns H.C. (1988) - The Early Toarcian (Jurassic) anoxic event: stratigraphic, sedimentary, and geochemical evidence. *American Journal of Science*, 288: 101-151.

Jenkyns H.C. (2003) - Evidence for rapid climate change in the Mesozoic - Paleogene greenhouse world. *Philolophical Transactions of Royal Society A*, 361: 1885-1916.

Jenkyns H.C. (2010) - Geochemistry of oceanic anoxic events. *Geochemistry, Geophysics, Geosystems,* 11, 3: 1-30.

Jenkyns H.C. & Clayton C.J. (1986) - Black shales and carbon isotopes in pelagic sediments from the Tethyan Lower Jurassic. *Sedimentology,* 33: 87-106.

Kemp D.B., Coe A.L., Cohen A.S. & Schwark L. (2005) - Astronomical pacing of methane release in the Early Jurassic period. *Nature,* 437: 396-399.

Léonide P., Floquet M., Durlet C., Baudin F., Pittet B. & Lécuyer C. (2012) - Drowning of a carbonate platform as a precursor stage of the Early Toarcian global anoxic event (Southern Provence sub-Basin, South-east France). *Sedimentology*, 59(1): 156-184.

Mattioli E. & Erba E. (1999) - Synthesis of calcareous nannofossil events in Tethyan Lower and Middle Jurassic successions. *Rivista Italiana di Paleontologia e Stratigrafia*, 105(3): 343-376.

Mattioli E., Pittet B., Bucefalo Palliani R., Rohl H.J., Schimd-Rohl A. & Morettini E. (2004) - Phytoplankton evidence for the timing and correlation of paleoceanographical changes during the early Toarcian oceanic anoxic event (Early Jurassic). *Journal of Geological Society of London*, 161: 685-693.

Mattioli E., Pittet B., Suan G. & Mailliot S. (2008) - Calcareous nannoplankton changes across the early Toarcian oceanic anoxic event in the western Tethys. *Paleoceanography*, 23: 1-17.

Mattioli E., Plancq J., Boussaha M., Duarte L.V. & Pittet B. (2013) - Calcareous nannofossil biostratigraphy: new data from the Lower Jurassic of the Lusitanian Basin. *Comunicaçoes Geològicas*, 100 (Especial I): 69-76.

McElwain J.C., Wade-Murphy J. & Hesselbo S.P. (2005) - Changes in carbon dioxide during an oceanic anoxic event linked to intrusion into Gondwana coals. *Nature*, 435: 479-482.

Medd A. W. (1971) - Some Middle and Upper Jurassic Coccolithophoridae from England and France. In: *Proceedings II Planktonic Conference,* Roma 1970, 2: 821-845. Institute of Geological Sciences, London.

Menini A., Mattioli E., Spangenberg, J.E., Pettit B. & Guillaume S. (2019) - New calcareous nannofossil and carbon isotope data for the Pliensbachian/Toarcian boundary (Early Jurassic) in the western Tethys and their paleoenvironmental implications. *Newsletter on Stratigraphy,* 52(2): 173-196.

Monechi S. & Thierstein H. R. (1985) - Late Cretaceous-Eocene nannofossil and magnetostratigraphic correlations near Gubbio, Italy. *Marine Micropaleontology*, 9(5): 419-440.

Morard A., Guex J., Bartolini A., Morettini E. & De Wever P. (2003). A new scenario for the Domerian-Toarcian transition. *Bulletin de la Société géologique de France*, 174(4), 351-356.

Pittet B., Suan G., Lenoir F., Duarte L.V., Mattioli E. (2014) - Carbon isotope evidence for sedimentary discontinuities in the lower Toarcian of the Lusitanian Basin (Portugal): Sea level change at the onset of the Oceanic Anoxic Event. *Sedimentary Geology*, 303: 1-14.

Röhl H.J. & Schmid-Röhl A. (2005) - Lower Toarcian (Upper Liassic) black shales of the Central European Epicontinental basin: a sequence stratigraphic case study from the SW German Posidonia Shale, Deposition of Organic-Carbon-Rich Sediments: Models, Mechanisms, and Consequences. *Society of Economic Paleontologists and Mineralogists Special Publication*, 82: 165-189.

Roth P.H. (1983) - Jurassic and Lower Cretaceous calcareous nannofossil in the Western North Atlantic (Site 534): biostratigraphy, preservation, and some observations on biogeography and paleoceanography. *Initial Reports Deep Sea Drilling Project,* 76: 587-621.

Stradner H. (1961) - Vorkommen von Nannofossilien im Mesozoikum und Alttertiär. *Erdöl-Zeitschrift*, 3: 77-88.

Svensen H., Planke S., Chevallier L., Malthe-Sørenssen A., Corfu F. & Jamtveit B. (2007) - Hydrothermal venting of greenhouse gases triggering Early Jurassic global warming. *Earth and Planetary Science Letters,* 256: 554-566.

Tintori A. (1977) - Toarcian fishes from the Lombardy Basin. *Bollettino della Società Paleontologica Italiana*, 16(2): 143-152.

Tremolada F., Van de Schootbrugge B.V. & Erba E. (2005) - Early Jurassic schizosphaerellid crisis in Cantabria, Spain: implications for calcification rates and phytoplankton evolution across the Toarcian oceanic anoxic event. *Paleoceanography*, 20: 1-11.

Van de Schootbrugge B., Richoz S., Pross J., Luppold F.W., Hunze S., Wonik T., Blau J., Meister C., Van de Meijst C. M. H., Suan G., Fraguas A., Fiebig J., Herrle J.O., Guex J., Little C.T.S., Wignall P.B., Püttmann W. & Oschmann W. (2019) - The Schandelah Scientific Drilling Project: A 25-million-year record of Early Jurassic palaeoenvironmental change from northern Germany. *Newsletter on Stratigraphy*, 52(3): 249-296.

Visentin S., Faucher G., Mattioli E. & Erba E. (2021a) - Taxonomic revision of the genus Carinolithus (Early-Middle Jurassic) based on morphometric analyses and diagenesis observations: Implications for biostratigraphy and evolutionary trends. *Marine Micropaleontology*, 162, 101950. https://doi.org/10.1016/j.marmicro.2020.101950.

Visentin S., Erba E. & Mutterlose J. (2021b) - Bio- and chemostratigraphy of the Posidonia Shale: a new database for the Toarcian Oceanic Anoxic Event from northern Germany. *Newsletter on Stratigraphy,* DOI: 10.1127/nos/2021/0658

Wignall P.B. (1991) - Model for transgressive black shales. *Geology*, 19(2): 167-170.